Applied Thermal Engineering 174 (2020) 115292

Contents lists available at ScienceDirect

Applied Thermal Engineering

journal homepage: www.elsevier.com/locate/apthermeng

Thermodynamic analysis of multi-heating cycles working around the critical point

Luis F. González-Portillo*, Javier Muñoz-Antón, José M. Martínez-Val

Universidad Politécnica de Madrid, José Gutiérrez Abascal, 2, 28006 Madrid, Spain

HIGHLIGHTS

- Multi-heating cycles supply heat at low temperature along the regenerator.
- Multi-heating increases exergy efficiency by reducing regenerator irreversibility.
- Exergy efficiency of multi-heating cycle is up to 24% greater than in simple cycle.
- Parametric analysis identifies the optimum conditions for multi-heating cycles.

ARTICLE INFO

Keywords:
Multi-heating
Pericritical
Supercritical
Transcritical
Heat management
Exergy efficiency

ABSTRACT

Multi-heating cycles reduce regenerator irreversibility, resulting in an increase of exergy efficiency. While a single heat source supplies the thermal power in simple regenerative cycles, in multi-heating cycles additional heat sources at lower temperatures supply part of this power along the regeneration. The greater the number of these additional heats, the higher the exergy efficiency is. An exergy analysis compares multi-heating and simple regenerative cycles working in the surroundings of the critical point. The main purpose is to identify the thermodynamic region in which there is a greater benefit of multi-heating, trying to abstract from the fluid as much as possible. The effect of compressor inlet temperature and limiting pressures is studied by means of parametric analysis. Cycles with the compressor working at pressures above the discontinuity line (set of coexistence line and Widom line) have small precooler irreversibilities and large regenerator irreversibilities. Multi-heating cycles take advantage of these conditions since they can reduce the regenerator irreversibilities and maintain the precooler irreversibilities small, leading to high exergy efficiencies. The results show that the exergy efficiency of multi-heating cycles may be up to 24% greater than in simple cycles.

1. Introduction

The use of supercritical fluids in power cycles have been proved as an alternative solution for high-performance power generation [1]. Cycles using supercritical fluids are commonly divided into two groups: transcritical and supercritical cycles. During last decades several layouts have been proposed for these two types of cycle with the purpose of increasing its efficiency [2].

The supercritical cycle was proposed by Feher [3]. Feher defined the supercritical cycle as a cycle working above the critical pressure with the compressor close to the critical point. These cycles can be classified as Brayton cycles since the working fluid is a gas. The power required by the compressor in supercritical cycles is small in comparison to standard Brayton cycles, but they conserve its simplicity and compactness [4]. Supercritical cycles are expected to benefit nuclear and solar power plants [5].

Feher [3] also considered the possibility of lowering the low-side pressure below the critical pressure but maintaining the high-side pressure above. These cycles are commonly called transcritical cycles [6]. They can be classified as Brayton cycles, when the working fluid is a gas, or Rankine cycles, when there is condensation in the low-pressure side. In the latter case, the working fluid in liquid state is compressed to a pressure above the critical pressure, heated without phase change, expanded in gas state and condensed back to the initial state. Most of these cycles include heat regeneration between the high- and the low-pressure sides. Angelino [7] studied these cycles with different configurations. It was found that transcritical cycles could exhibit greater efficiency than reheat steam cycles. Since then several researchers have analysed transcritical cycles in different fields such as solar energy [8], waste heat recovery [9] or biomass [10].

* Corresponding author.
E-mail address: lf.gonzalez@upm.es (L.F. González-Portillo).

https://doi.org/10.1016/j.applthermaleng.2020.115292
Received 4 October 2019; Received in revised form 20 January 2020; Accepted 5 April 2020
Available online 11 April 2020
1359-4311/

Nomenclature

c_p	specific heat at constant pressure
CO_2	carbon dioxide
DL	discontinuity line
e	exergy
f_p	logarithmic factor of isobaric expansion
h	specific enthalpy
HTR	high-temperature regenerator
i	Irreversibility
IHX	intermediate heat exchanger
LTR	low-temperature regenerator
P	pressure
q	heat
r	compression ratio
s	specific entropy
T	temperature
T_m	pinch point temperature
w	specific work
z	compressibility factor

Greek letters

ε	effectiveness
η	efficiency
τ	Carnot factor ($\tau = T_{t,in}/T_{c,in}$)

Subscripts

ah	additional heat
amb	ambient
c	compressor
C	Carnot
cr	critical
e	exergy
H	high
HP	high pressure
in	inlet
L	low
LP	low pressure
max	maximum
out	outlet
pc	precooler
ph	primary heat
R	ideal gas constant
r	reduced
reg	regeneration
s	constant entropy
t	turbine
th	thermal

Some authors compare the differences between transcritical and supercritical cycles [6,11], but most of researchers analyse only either the transcritical [12,13] or the supercritical [14,15] layout, although the limits between them are not clear sometimes. Previous work from the authors of this paper [16] analysed the similarities of transcritical and supercritical cycles, agglutinating all the cycles working around the critical point under the name of pericritical cycles, where “peri” stands for “around” in Latin. The characterization of these cycles was made under a unique analysis, avoiding differentiation between transcritical and supercritical. The main difference between the behavior of pericritical cycles was found in the position of the compressor with respect to the so called discontinuity line, which will also be used in this work.

The discontinuity line is the set of the coexistence line (or biphasic bell) and the Widom line, i.e., it is the line that separates the regions of liquid and gas behavior. The coexistence line is well known for separating these two regions [17]. The Widom line, introduced by Sciortino in 1997 [18], separates the regions of liquid-like and gas-like in a continuous manner when the fluid pressure is above the critical pressure [19]. The behavior of the fluid crossing the Widom line is very

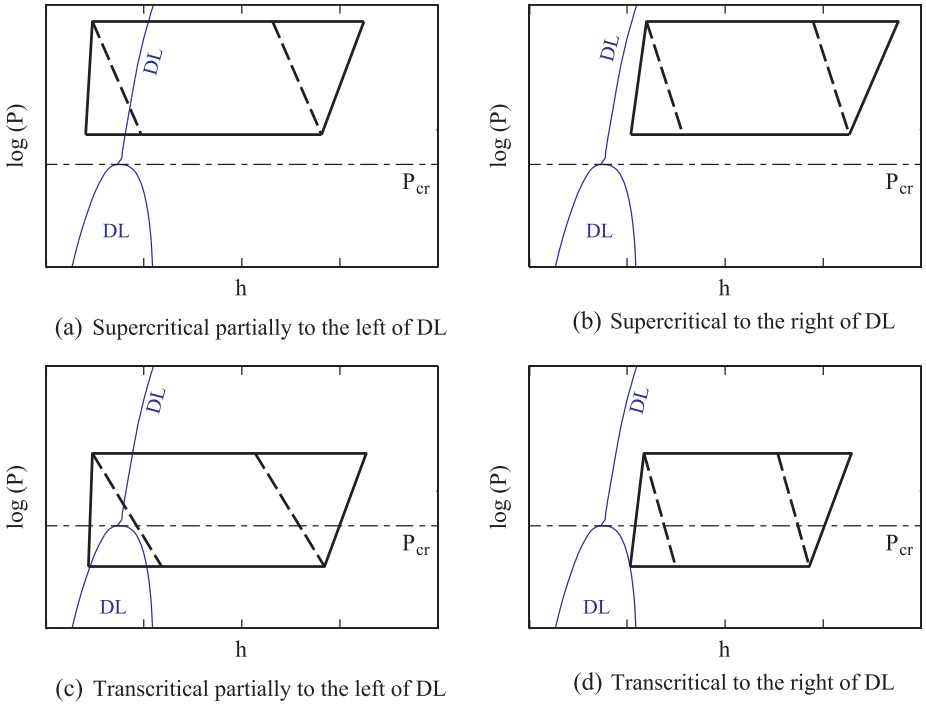

Fig. 1. Pericritical cycles and discontinuity line (DL) in P-h diagram.

similar to the behavior of the fluid crossing the coexistence line, but with softer property variations [20].

Fig. 1 shows four examples of pericritical cycles. Fig. 1a and b would be commonly called supercritical and Fig. 1c and d would be called transcritical. The compressor is located to the left of the discontinuity line (DL) in Fig. 1a and 1c, and to right in Fig. 1b and d. The low-pressure side experiences phase change in Fig. 1c because it crosses the part of the discontinuity line corresponding to the biphasic bell, and it experiences pseudo phase change in Fig. 1a because it crosses the part of the discontinuity line corresponding to the Widom line. The whole cycle is in gaseous state in the cases of Fig. 1b and d.

Some pericritical cycles exhibit large internal irreversibility in the regenerator due to the mismatch between the specific heats of low- and high-pressure sides [21]. This problem is commonly solved by adding a second compressor to the cycle, which recompresses part of the fluid [22]. In a recompression cycle, the regenerator is divided into two parts. The recompression manages the flow rates to reduce the regenerator irreversibility. Despite the extra compression work, these cycles achieve higher efficiencies than standard regenerative transcritical and supercritical cycles [22]. Due to its high efficiencies, recompression cycles have been reported as potential replacements of Rankine cycles in thermal power plants with high-temperature heat sources [23].

This paper analyses a different way to reduce the regenerator irreversibility: the multi-heating cycle. It consists in supplying additional heats at low-medium temperature to the high-pressure side during the heat regeneration. These heats replace part of the heat supplied by the primary heat source, which involves heat sources at lower average temperature. Multi-heating cycles have been previously studied with different names [6,24]. Syblik et al. [24] analyse the thermal efficiency of these cycles with supercritical CO_2. The results show that there are other layouts with higher thermal efficiencies. Kim et al. [6] show that the advantage of multi-heating cycles lays in the exergy efficiency. One supercritical CO_2 cycle and one transcritical CO_2 cycle are analysed, showing higher exergy efficiency in the case of multi-heating cycle than in the case of simple cycle.

The main purpose of this work is to identify the thermodynamic region in which there is a greater exergetic benefit for multi-heating. In order to do so, the analysis tries to abstract from the fluid as much as possible and so focus on the cycle position within the thermodynamic diagram. In this way, different operating conditions can be analysed that, otherwise, would be imposed by the fluid. An exergy analysis, guided by the discontinuity line, compares pericritical simple cycles and pericritical multi-heating cycles. In a similar way to our previous work [16] (focused on analyzing the features of simple pericritical cycles), the discontinuity line helps to characterize multi-heating cycles. This novel method opens a new field of study for the optimization of pericritical cycles. Moreover, this is the first study, to the best of our knowledge, to analyse multi-heating cycles for different operating conditions, which can be applied thanks to the fluid abstraction.

The exergy efficiency of multi-heating and simple cycles will be compared for different operating conditions. The models used to simulate these cycles are explained in Section 2. The exergy efficiency and the irreversibilities for a specific multi-heating cycle are analysed in Section 3. Section 4 studies the optimum multi-heating configurations for different operating conditions and for different fluids. Conclusions close the paper in Section 5.

2. Simple and multi-heating pericritical cycles

2.1. Simple cycles

Fig. 2 shows the configuration of a simple pericritical cycle. If the compressor worked in liquid state, compressor and precooler would normally be called pump and condenser, respectively. However, since the fluid in the compressor may be in different states depending on the pericritical cycle, these two components will be called compressor and precooler in order to generalize.

Fig. 3 shows a simple regenerative pericritical cycle in P-h and T-s diagrams. The cycle is represented with low-side pressure in the critical pressure. The purpose is to remind that pericritical cycles can have the low-side pressure above or below the critical pressure. Moreover, the compressor inlet temperature is, in this case, below the critical temperature. Nonetheless, it must be remembered that it could be above.

Eqs. (2.1)–(2.5) represent the different phases of the cycle by means of enthalpy difference. These phases are: compression work (w_c), regenerator heat exchange (q_{reg}), primary heat (q_{ph}), turbine work (w_t), heat released by the precooler (q_{pc}).

$$w_c = h_2 - h_1 \tag{2.1}$$

$$q_{reg} = h_3 - h_2 = h_5 - h_6 \tag{2.2}$$

$$q_{ph} = h_4 - h_3 \tag{2.3}$$

$$w_t = h_4 - h_5 \tag{2.4}$$

$$q_{pc} = h_6 - h_1 \tag{2.5}$$

The thermal efficiency is the ratio of net work and heat supplied by the heat source:

$$\eta_{th} = \frac{w_t - w_c}{q} \tag{2.6}$$

The cycle will be limited by the compressor and turbine inlet temperatures, $T_{c,in}$ and $T_{t,in}$, and the high- and low-side pressures, P_H and P_L. The pressure will decrease along the cycle. The pressure drop will imply that the turbine pressure ratio will be lower than the compressor pressure ratio. The fractional pressure drop, $\Delta P_{drop}/P$, will be defined in this analysis as:

$$\Delta P_{drop}/P = \frac{P_H - P_4}{P_H} \tag{2.7}$$

Compressor and turbine inlet pressures and temperatures define points 1 and 4. Points 2 and 5 are determined by means of the compressor and turbine efficiencies, η_c and η_t:

$$\eta_c = \frac{h_{2,s} - h_1}{h_2 - h_1} \tag{2.8}$$

$$\eta_t = \frac{h_4 - h_5}{h_4 - h_{5,s}} \tag{2.9}$$

The low-pressure side of the cycle between points 6–5 heats the high-pressure side between points 2–3 through an intermediate heat exchanger (IHX). Each small part i of this IHX must fulfil the following enthalpy balance:

$$c_{P,HP,i}\Delta T_{HP,i} = c_{P,LP}\Delta T_{LP,i} \tag{2.10}$$

where c_p is the specific heat and ΔT the temperature increment of the

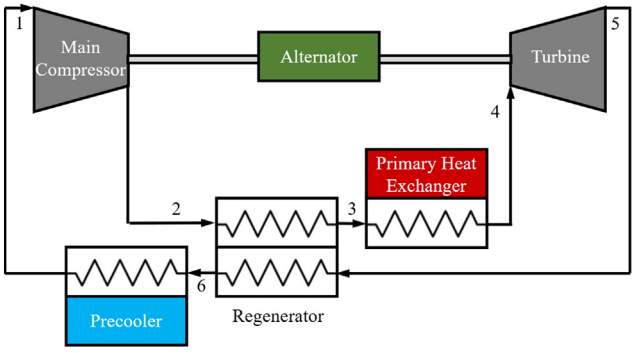

Fig. 2. Diagram of a simple regenerative pericritical cycle (inspired by Dyreby [25]).

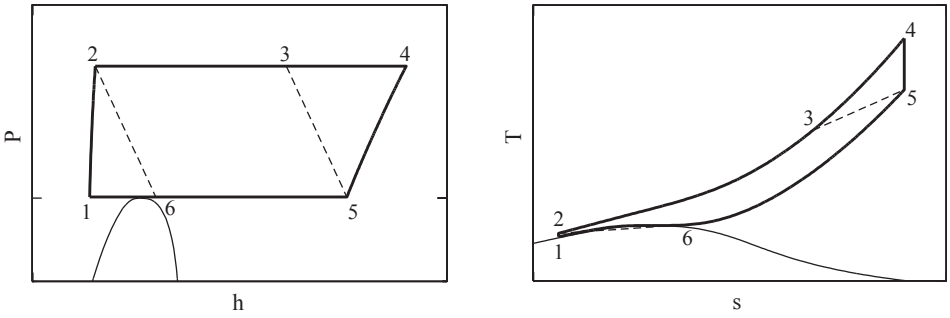

Fig. 3. Example of regenerative pericritical cycle in diagrams P-h and T-s.

high-pressure (*HP*) and low-pressure (*LP*) parts *i* of the IHX.

Fig. 4 shows the value of the dimensionless specific heat c_p/R as a function of the reduced temperature ($T_r = T/T_{cr}$) for different reduced pressures ($P_r = P/P_{cr}$). The balance from Eq. (2.10) involves that the temperature increment ΔT will have two tendencies:

- $\Delta T_{HP,i} > \Delta T_{LP,i}$ when $c_{P,HP,i} < c_{P,LP}$
- $\Delta T_{HP,i} < \Delta T_{LP,i}$ when $c_{P,HP,i} > c_{P,LP}$

The point separating these two tendencies (i.e, where the two specific heats, c_p, are equal) has the minimum temperature difference between the high- and the low-pressure sides. This point is called pinch point. The temperature at which the pinch point appears, T_m, depends on the limiting pressures of the cycle. In a pericritical cycle, the pinch point may appear at the IHX inlet of the high-pressure part (point 2), or in middle of the IHX.

If the IHX were infinitely large, the temperature difference between the high- and the low-pressure sides in the pinch point would be zero, and the heat exchanged would be the maximum possible, $\Delta h_{reg,\max}$. The effectiveness, ε, will define how much heat, Δh_{reg}, a real IHX exchanges in comparison to the maximum possible, $\Delta h_{reg,\max}$:

$$\varepsilon = \frac{\Delta h_{reg}}{\Delta h_{reg,max}} \tag{2.11}$$

The part of the heat that the low-pressure side cannot supply to the high-pressure side will be supplied by the heat source. A large part of the heat needed in pericritical cycles comes from the specific heat mismatch in the IHX from Eq. (2.10). This mismatch is dragged along the regeneration, resulting in a greater amount of heat supplied by the heat source [16]. The purpose of multi-heating cycles is to reduce the heat due to the mismatch of specific heat.

2.2. Multi-heating cycles

The specific heat imbalance from Eq. (2.10) involves a greater temperature increment in the low-pressure side than in the high-pressure side. A way of equalizing the temperature increment in the low- and the high-pressure sides is by supplying additional heat to compensate the mismatch of specific heat. Eq. (2.12) represents the energy balance needed to obtain the same temperature increment ΔT in both pressure sides in a section *i* of the IHX. Note that the additional heat, $q_{ah,i}$, has to be supplied in the part of the regenerator where $c_{P,HP,i} > c_{P,LP}$, i.e., at temperatures $T > T_m$.

$$c_{P,HP,i}\Delta T_{HP,i} = c_{P,LP}\Delta T_{LP,i} + q_{ah,i} \tag{2.12}$$

The result would be that infinite additional heats, $q_{ah,i}$, at different temperatures, T_i, balance the regenerator. The value of each additional heat will depend on the specific heat difference between the low and high-pressure sides.

Fig. 5 shows P-h and T-s diagrams of a pericritical cycle with the proposed additional heats during the regeneration. The small arrows represent the infinite additional heats and the big arrow represents the primary heat. The red dashed lines indicate the heat regeneration limits. Point 3′ marks the end of regeneration in the high-side pressure when there are additional heats, while point 3 marked this end in the simple cycle. This involves a reduction of the primary heat. The part to the left of the pinch point (T_m), is common to cycles with and without additional heats.

Note that the pinch point (T_m) in Fig. 5 is in the middle of the regeneration. Thus, additional heats are only supplied in the part of the regeneration whose temperature is above T_m. However, if the pinch point were in the compressor outlet (point 2) then all the additional heats would be supplied along the whole regeneration.

The supply of infinite additional heats is useful as theoretical explanation about how to balance the regenerator in pericritical cycles. However, it would be impossible to carry out in reality. A real alternative to balance the regenerator is proposed and analysed: the multi-heating cycle. Besides the primary heat, the multi-heating cycle supplies additional heats in the middle of the regeneration. Fig. 6 shows the diagram of a multi-heating cycle.

The multi-heating cycle from Fig. 6 has two heat supplies: the primary heat, q_{ph}, and the additional heat, q_{ah}, defined as:

$$q_{ph} = h_4 - h_{3'} \tag{2.13}$$

$$q_{ah} = h_{8'} - h_{7'} \tag{2.14}$$

The high-pressure flow exiting the compressor goes through a first regenerator to exchange heat with the low-pressure part about to enter the precooler. This regenerator covers the part where the pinch point appears. The additional heat is supplied after this first regeneration up to a certain temperature corresponding with point 8′. More additional heats could be supplied at higher temperatures afterwards. In this way, the gap shown in Fig. 6 could be filled with more dashed-line boxes. If

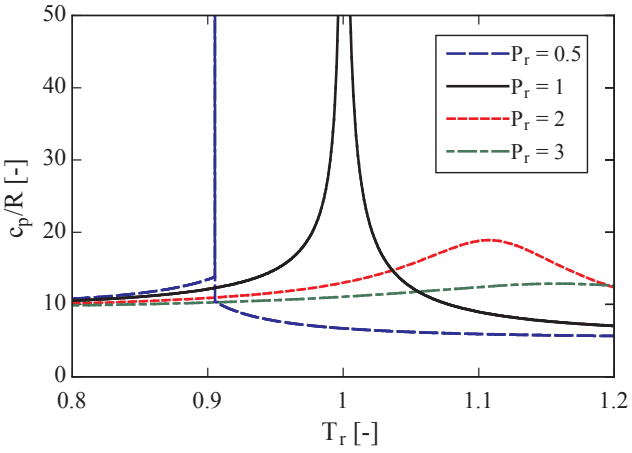

Fig. 4. Dimensionless specific heat, c_p/R, as a function of the reduced temperature, T_r, for different reduced pressures.

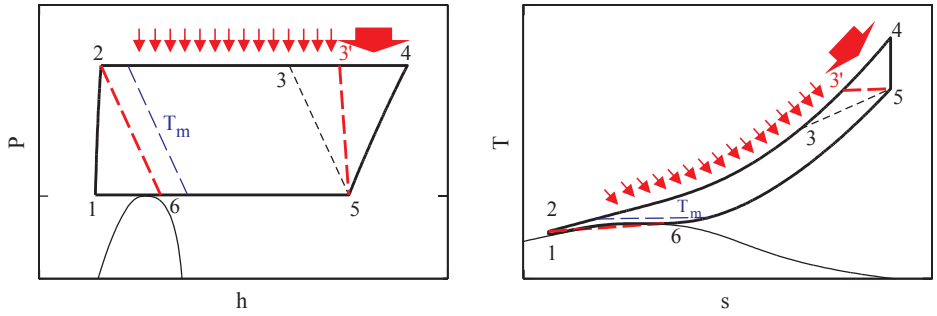

Fig. 5. Scheme of a pericritical cycle with infinite additional heats supplied during the regeneration in diagrams P-h and T-s.

the temperature of the last additional heat is not the turbine outlet temperature, then a last regenerator is needed before the primary heat exchanger.

The problem of providing additional heats must be solved according to the available heat sources. Each new additional heat may be supplied to the cycle by means of a different heat source. An option would be to use solar thermal power, where the heat carrier fluid can carry the heat within a selected range of temperatures, according to solar conditions, concentrator field, and receiver features [26].

Fig. 7 shows P-h and T-s diagrams of a regenerative multi-heating cycle with one additional heat. The red dashed lines indicate the heat regeneration limits in a multi-heating cycle, and the black dashed line in a simple cycle. The lines limiting the two regenerators in the P-h diagram are parallel due to the energy balance. Therefore, after the additional-heat supply (line 7′-8′), the regeneration limiting lines 8′-9′ and 3′-5 are more vertical, allowing higher temperatures in the high-pressure side of the regenerator. Thus, the primary heat (line 3′-4) in a multi-heating cycle is reduced.

The total heat supplied to the cycle will depend on the capacity to recuperate heat of the intermediate heat exchangers. This capacity was defined by the effectiveness of the regenerator in Eq. (2.11). This effectiveness will also be used to define the global regeneration phase in multi-heating cycles. Thus, this global effectiveness defines the regeneration in the low-pressure side, regardless of what happens in the high-pressure side. The idea of defining a global effectiveness has been previously used by Padilla et al. [27] in cycles where there is more than one regenerator. This allows the comparison between simple regenerative cycles and cycles with modifications inside the cycle, such as the proposed multi-heating cycles.

Besides the global effectiveness, the effectiveness of the high-temperature regenerator (HTR) is used to complete the definition of the regeneration. Eq. (2.11) will also be used to define this effectiveness. The two mentioned effectiveness (global and HTR) and the highest temperature of the additional heat will define the inside of the multi-heating cycle. If more additional heats are supplied at different temperature, a new effectiveness and heat temperature will be needed to define each new additional heat.

If we consider the diagram from Fig. 7 with the points 1245 already defined, point 6 will be calculated by means of the global effectiveness. This implies that a regenerative cycle with or without additional heats and the same global effectiveness will have the same point 6, i.e., the precooler will extract the same heat. The heat temperature defines point 8′ and the HTR effectiveness points 9′ and 3′. The definition of point 9′ determines point 7′ due to the energy balance between lines 2–6 and 7′–9′. This means that the effectiveness of the low-temperature heat exchanger will be obtained as a result, always fulfilling the requirement of having a minimum temperature difference.

A simple balance of energy in the regenerators proves that a cycle with the same points 1245 and the same global effectiveness will need the same amount of heat, either if there is additional heat or not. This means that the total heat supplied in a simple cycle would be the same than the total heat supplied in a multi-heating cycle (except that in this case the total heat is the sum of primary heat, q_{ph}, and additional heat, q_{ah}). Thermal efficiency would also be the same according to Eq. (2.10).

Multi-heating cycles and simple regenerative cycles with the same points 1245 and the same global effectiveness have the same thermal efficiency. The main difference is the temperature of the heat supply, specifically, the temperature of the additional heat. The exergy measures the cost of the heat source [28], relating it with the heat source temperature. An exergetic analysis will appreciate the benefits of the cycle with additional heats during regeneration.

3. Exergy analysis of multi-heating cycles

The maximum work from a Carnot engine supplied with a heat, q, operating between a heat source and a heat sink at temperatures T_{hot} and T_{cold}, respectively, is expressed in Eq. (3.1) [6]. This work will be the exergy input, e_{in}, to the cycle.

$$e_{in} = q \cdot \eta_C = q\left(1 - \frac{T_{cold}}{T_{hot}}\right) \tag{3.1}$$

The exergy input of each heat source depends on the supplying

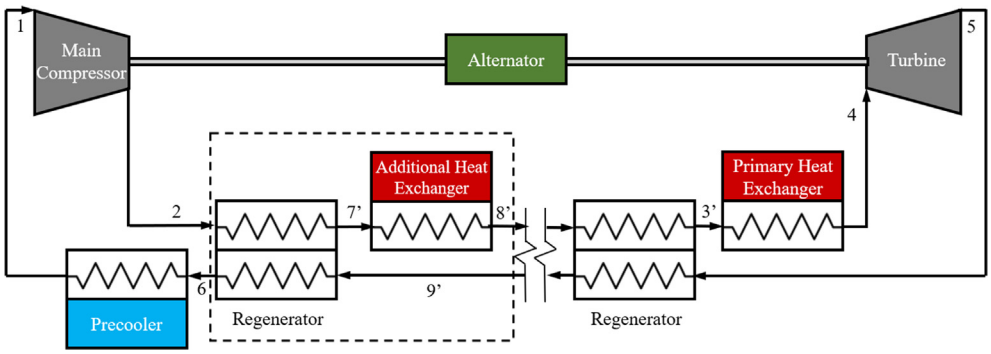

Fig. 6. Diagram of a regenerative multi-heating cycle (inspired by Dyreby [25]).

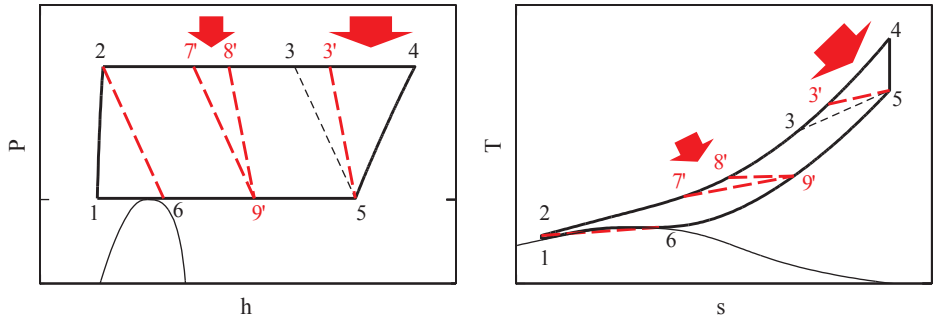

Fig. 7. Scheme of a multi-heating cycle with one additional heat in diagrams P-h and T-s.

temperature. Thus, the heats added in multi-heating cycles will have different exergy inputs depending on the heat source temperature. In order to generalize the analysis and avoid the definition of the heat source, the heat source temperature is considered the maximum temperature of the heat. In the same way, the heat sink temperature will be minimum temperature of the cycle. Thus, heats in Fig. 7 would be defined by temperatures $T_{8'}$ and T_4, and the heat sink by temperature T_1.

The total exergy input of a cycle with several additional heats will be the sum of the exergy input of each heat. The heat supplied at the maximum temperature will have higher specific costs (in terms of Carnot efficiency, η_c) than the rest of the heats. Therefore, reducing this heat and substituting it by additional heats at lower temperatures will reduce the total exergy input.

An exergy analysis will guide the study of multi-heating cycles, based in the comparison with the simple cycle. The computational models are developed in EES (Engineering Equation Solver) [29], which provides built-in thermophysical property data. The calculations use the thermodynamic properties of CO_2, but the variables pressure and temperature are expressed in its reduced form ($P_r = P/P_{cr}$ and $T_r = T/T_{cr}$). In this way, the major trends identifying the features of each thermodynamic region can be extrapolated to other fluids able to work in that region.

The parameters from Table 3.1 are used in the exergy analysis of this section. Reduced pressures and temperatures are selected to have a cycle with the compressor working at pressures above the discontinuity line. This cycle will have low compression work and high irreversibilities in the regeneration [16]. In this way, the benefit of multi-heating (increase the exergy efficiency by reducing these irreversibilities) will be easily identified. Isentropic efficiencies, effectiveness and pressure drop are values from the literature referenced in the table. The fractional pressure drop is the sum of all the pressure drops in the cycle from [4].

Fig. 8 shows the exergy inputs of the primary heat, $e_{in,ph}$, additional heat, $e_{in,ah}$, and total heat, $e_{in,total}$, as a function of the additional-heat temperature, T_{ah}. Exergy and temperature are expressed in dimensionless way. The exergy input of the additional heat increases with the temperature and the primary heat exergy input decreases. The decrease of the primary heat exergy is produced by the increase of the additional heat. Most of the additional heat can be supplied at temperatures under $T_r = 1.5$ due to the larger specific heat mismatch up to this temperature. This means that increasing the additional-heat temperature up to this temperature strongly reduces the primary heat, and so its exergy input. Moreover, it involves an increase in the exergy input of the additional heat, but the low Carnot efficiencies reduce its impact. The combination of the exergies results in a total exergy input with a minimum in its curve at a temperature $T_{ah,r} = 1.45$.

The relation between the generated work and the exergy input is analysed by means of the second law efficiency:

$$\eta_{ex} = \frac{w_t - w_c}{e_{in,total}} = \frac{w_t - w_c}{\sum e_{in,j}} \tag{3.2}$$

where $e_{in,j}$ is the exergy input of each heat supplied to the cycle at a different temperature, including the main heat source.

The multi-heating cycle studied in Fig. 8 has constant compressor and turbine works. Therefore, the minimum exergy input defines the maximum exergetic efficiency. The point with the minimum exergetic efficiency to the left of Fig. 8 corresponds to a cycle with no additional heat. The other end (to the right) of the exergetic efficiency curve represents a cycle with the additional heat supplied at the minimum temperature of the primary heat.

The exergy efficiency can also be expressed as a function of the exergy losses (or irreversibilities) of each component, i_j:

$$\eta_{ex} = 1 - \sum \frac{i_j}{e_{in,total}} = 1 - i_{r,j} \tag{3.3}$$

The exergy loss is defined as the input exergy minus the outlet exergy, and the specific exergy of a point, e_j, is expressed as:

$$e_j = h_j - h_{amb} - T_{amb}(s_j - s_{amb}) \tag{3.4}$$

where the subscript *amb* stands for ambient conditions, which are assumed to be the heat sink conditions.

The following equations express the irreversibility of the components of a multi-heating cycle with one additional heat such as the one shown in Fig. 7:

$$i_c = w_c - (e_2 - e_1) \tag{3.5}$$

$$i_t = (e_4 - e_5) - w_t \tag{3.6}$$

$$i_{LTR} = (e_{9'} - e_6) - (e_{7'} - e_2) \tag{3.7}$$

$$i_{HTR} = (e_5 - e_{9'}) - (e_{3'} - e_{8'}) \tag{3.8}$$

$$i_{ph} = e_{in,ph} - (e_4 - e_{3'}) \tag{3.9}$$

$$i_{ah} = e_{in,ah} - (e_{8'} - e_{7'}) \tag{3.10}$$

$$i_{pc} = e_6 - e_1 \tag{3.11}$$

Fig. 9 shows the irreversibilities of a multi-heating cycle with one additional heat at conditions of Table 3.1 as a function of additional-heat temperature, T_{ah}. While irreversibilities of precooler, compressor and turbine barely depend on additional-heat temperature,

Table 3.1
Parameters used to analyze multi-heating pericritical cycles.

Parameter	Value
Reduced high-side pressure, $P_{H,r}$	3
Reduced low-side pressure, $P_{L,r}$	1
Reduced compressor inlet temperature, $T_{c,in,r}$	0.9
Carnot factor, $\tau = T_{t,in}/T_{c,in}$	3
Compressor efficiency, η_c [30]	0.85
Turbine efficiency, η_t [30]	0.85
IHX effectiveness, ε [27]	0.95
Fractional pressure drop, $\Delta P_{drop}/P$ [4]	0.05

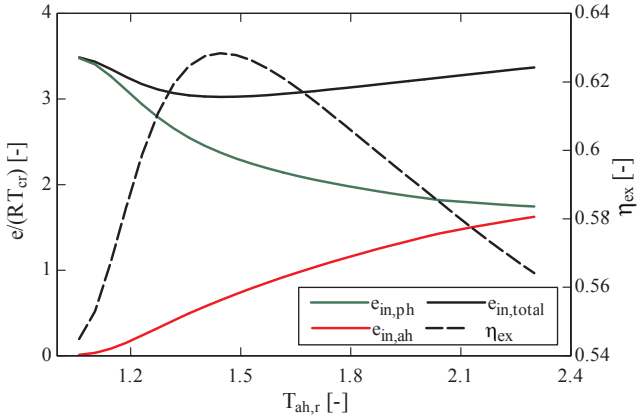

Fig. 8. Exergy inputs of the primary heat, $e_{in,ph}$, additional heat, $e_{in,ah}$, and total heat, $e_{in,total}$, and cycle exergy efficiency, η_{ex}, as a function of the additional-heat temperature, T_{ah}.

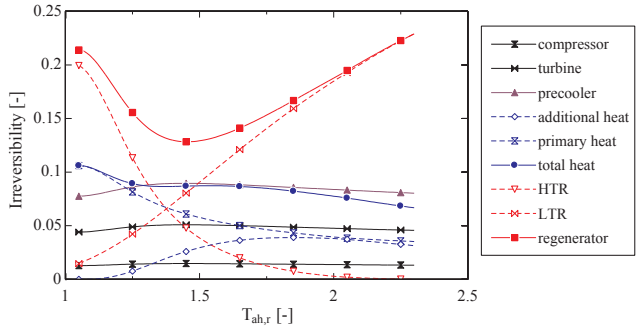

Fig. 9. Irreversibility of the components of a multi-heating cycle as a function of additional-heat temperature, T_{ah}.

irreversibilities of the heats (primary and additional) and regenerators (HTR and LTR) are highly dependent.

The additional-heat irreversibility to the left of Fig. 9 is zero because there is no additional heat, i.e., it is a simple cycle. This irreversibility increases with the additional-heat temperature, T_{ah}, while the primary heat irreversibility decreases. The result is a total-heat irreversibility that hardly depends on additional-heat temperature.

The irreversibilities of the heats would be larger if greater heat source temperatures were considered. This means that the total irreversibility curve could change. The precooler irreversibility would be also greater if a lower heat sink temperature were used to calculate the exergy loss. However, the heat sink irreversibility would still be almost constant and therefore it would not affect the behavior of the total irreversibility curve.

The LTR irreversibility increases almost linearly with the temperature, while the HTR irreversibility decreases exponentially. LTR and HTR irreversibilities experience the largest variations, which implies a greater impact in the exergy efficiency than the rest of the cycle components. The result is that the point of minimum exergy loss is achieved by reducing the total irreversibility of the regeneration. The regenerator irreversibility (sum of HTR and LTR) is minimized at temperature $T_{ah,r} = 1.45$, which corresponds to the temperature of minimum total irreversibility (or maximum exergy efficiency). Note that the irreversibility in a heat exchanger is given by the variation of entropy. Thus, reducing the entropy in the regeneration of multi-heating cycles increases the exergy efficiency.

The irreversibility of regeneration is highly reduced at temperature $T_{ah,r} = 1.45$. However, it is still the largest one. The supply of more additional heats will reduce even more this irreversibility, resulting in higher exergy efficiencies. Fig. 10 shows the exergy efficiency, η_{ex}, of multi-heating cycles with up to six additional heats. The temperature of each additional heat is calculated to maximize the exergy efficiency.

Supplying more additional heats increases exergetic efficiency. However, this increase lowers with the number of additional heats. The relative increase of supplying one additional heat with respect to the simple case (no additional heat) is 16%. The relative increase of supplying a second additional heat is 6% and if a third additional heat is supplied then this increase is only 3%. While a greater number of additional heats involves higher exergy efficiency, it also involves a more complex system, and so more expensive. Next section analyses the best conditions for multi-heating cycles with one additional heat.

4. Best conditions for multi-heating cycles

This section characterizes multi-heating cycles according to the compressor position in the thermodynamic diagram. Thermodynamic properties of CO_2 are used for the calculations. However, the cycle characterization attempts to abstract from the fluid as much as possible by using reduced pressure ($P_r = P/P_{cr}$) and reduced temperature ($T_r = T/T_{cr}$). In this way, critical pressure and critical temperature are irrelevant in the analysis.

The purpose of this section is to find the thermodynamic regions in which multi-heating cycles involve a greater improvement with respect to simple regenerative cycles. The discontinuity line will have a great impact in determining these thermodynamic regions. This line separates liquid and gas behaviors both below and above the critical pressure. The discontinuity line is defined as the line that consists of points with maximum value of f_P for each pressure, where f_P is defined in Eq. (4.1) [16,31].

$$f_P = \left(\frac{\partial Lnz}{\partial LnT}\right)_P \tag{4.1}$$

All cycles in the analysis will have a Carnot factor $\tau = 3$ ($\tau = T_{t,in}/T_{c,in}$). In this way, the Carnot efficiency will be the same: $\eta_C = 2/3$. Efficiencies, effectiveness and pressure drop will be those from Table 3.1. The variables of the analysis will be compressor inlet temperature, high- and low-side pressures, and additional-heat temperature.

4.1. Compressor inlet

Compressor inlet temperature and low-side pressure determine the compressor inlet position in the thermodynamic diagram. Fig. 11 shows six different simple pericritical cycles in a P-h diagram working with a high pressure $P_{H,r} = 3$ and different compressor inlet positions. Three of these cycles have the compressor working to the left of the discontinuity line (DL) and the other three to the right.

The position of the compressor inlet with respect to the

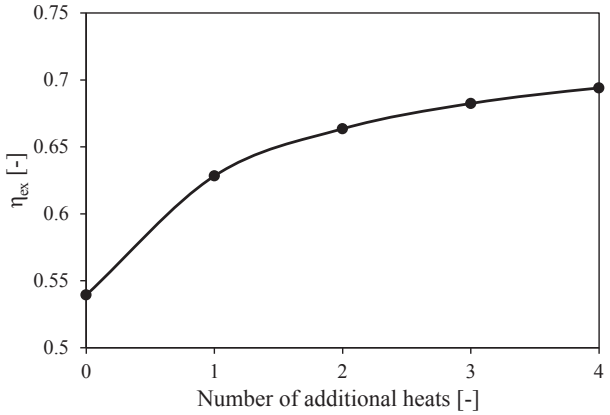

Fig. 10. Exergy efficiency, η_{ex}, of multi-heating cycle as a function of number of additional heats.

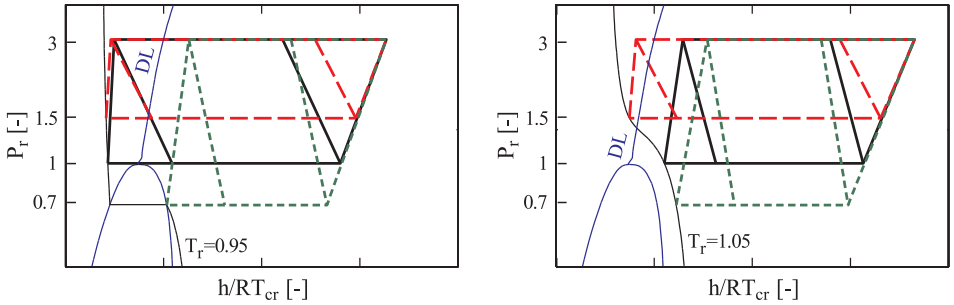

(a) $T_{c,in,r} = 0.95$ (b) $T_{c,in,r} = 1.05$

Fig. 11. P-h diagram of simple pericritical cycles working with high-side pressure $P_{H,r} = 3$ and different low-side pressures and compressor inlet temperatures (a) $T_{c,in,r} = 0.95$ and (b) $T_{c,in,r} = 1.05$.

discontinuity line determines the cycle behavior. Fig. 12 shows the irreversibilities of all components in a simple cycle with high-side pressure $P_{H,r} = 3$ as a function of low-side pressure. Cycles from Fig. 12a have compressor inlet temperature $T_{c,in,r} = 0.95$ and cycles from Fig. 12b $T_{c,in,r} = 1.05$. Lines $DL_{0.95}$ and $DL_{1.05}$ indicate the point where the compressor inlet crosses the discontinuity line at temperatures $T_r = 0.95$ and $T_r = 1.05$, respectively. These lines separate the low-side pressures into two regions: above and below the discontinuity line.

The behavior of the regions above and below the discontinuity line is similar in Fig. 12a and b. Simple pericritical cycles with the low-side pressure above the discontinuity line have large regeneration irreversibilities. This irreversibility decreases when the low-side pressure falls below the discontinuity line. This decrease is abrupt when the compressor inlet temperature is $T_{c,in,r} = 0.95$ and softer when the temperature is $T_{c,in,r} = 1.05$. The irreversibility continues going down at lower pressures. At low-side pressure $P_{L,r} = 0.5$ there is hardly regeneration irreversibility.

The larger the regeneration irreversibilities the greater the potential of multi-heating is. Therefore, cycles with the low-pressure side above the discontinuity line will have greater potential to exploit multi-heating. Fig. 13 shows the irreversibilities of several multi-heating cycles with different compressor inlet conditions as a function of additional-heat temperature. The leftmost point of each curve represents the irreversibility in a simple cycle (the additional-heat temperature is the compressor outlet temperature and, therefore, the additional-heat is zero).

Figures a, b and c have the compressor inlet pressure above the discontinuity line, and figures d, e and f below. The regenerator irreversibility is the largest one in figures a, b and c, and it can be highly reduced by means of an additional heat at temperature T_{ah}. The result is a reduction in the total irreversibility.

When the low-side pressure is very low (figures e and f), the precooler irreversibility is the largest one, and the regenerator irreversibility is almost null. An additional heat at temperature T_{ah} hardly affects the total irreversibility.

The compressor inlet in the cycle of Figure d is also below the discontinuity line, such as in figures e and f. However, precooler and regenerator irreversibilities are similar in this case. The additional heat gets to reduce the total irreversibility, but less than in figures a, b and c, where the compressor inlet pressure is above the discontinuity line.

The compressor inlet temperature in Figure d is above the critical temperature ($T_{c,in,r} > 1$). Thus, the low-side pressure that crosses the discontinuity line is above the critical pressure ($P_{L,r} > 1$) and the irreversibility variation through the different values of low-side pressure is continuous. If the low-side pressure is below the discontinuity line, but close, then the regenerator irreversibility is still high, and multi-heating can reduce it.

Cycle irreversibility can be used to calculate the exergy efficiency (see Eq. (3.3)). Fig. 14 shows the exergy efficiency, η_{ex}, of simple and a multi-heating cycles as a function of low-pressure side, $P_{L,r}$. The additional-heat temperature has been optimized in all the multi-heating cycles to maximize the exergy efficiency. The high-side pressure is still $P_{H,r} = 3$ in all cases. The compressor inlet temperature in the cycles of Fig. 14a and b are $T_{c,in,r} = 0.95$ and $T_{c,in,r} = 1.05$, respectively.

The maximum exergy efficiency of the simple cycle in Fig. 14a is obtained at a compressor inlet pressure just above the discontinuity line. The small precooler irreversibility outweighs the large regeneration irreversibility (see Fig. 12a). The multi-heating cycle may reduce this regeneration irreversibility. Thus, the maximum exergy efficiency of multi-heating cycle is obtained at the same low-side pressure than for the simple cycle.

The maximum exergy efficiency in Fig. 14b is obtained at different low-side pressures in simple and multi-heating cycles. The optimum configuration for the simple cycle ($P_{L,r} \approx 1$) has similar inefficiencies in precooler and regenerator (see Fig. 12b). Raising the low-side pressure in the simple cycle involves a smaller precooler irreversibility, but also

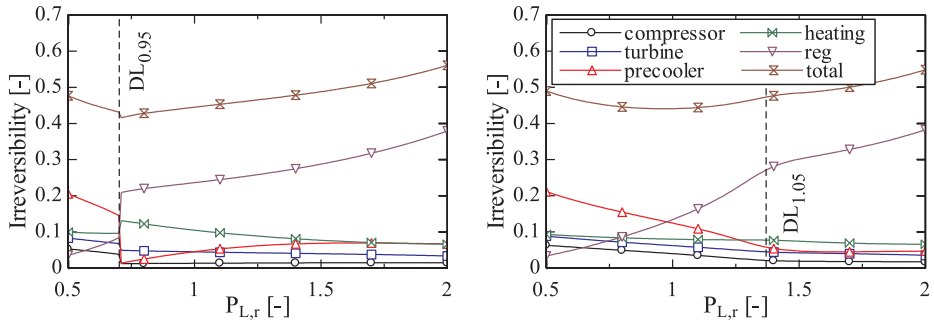

(a) $T_{c,in,r} = 0.95$ (b) $T_{c,in,r} = 1.05$

Fig. 12. Irreversibilities as a function of the low-side pressure, $P_{L,r}$, in simple pericritical cycles with a compressor inlet temperature (a) $T_{c,in,r} = 0.95$ and (b) $T_{c,in,r} = 1.05$.

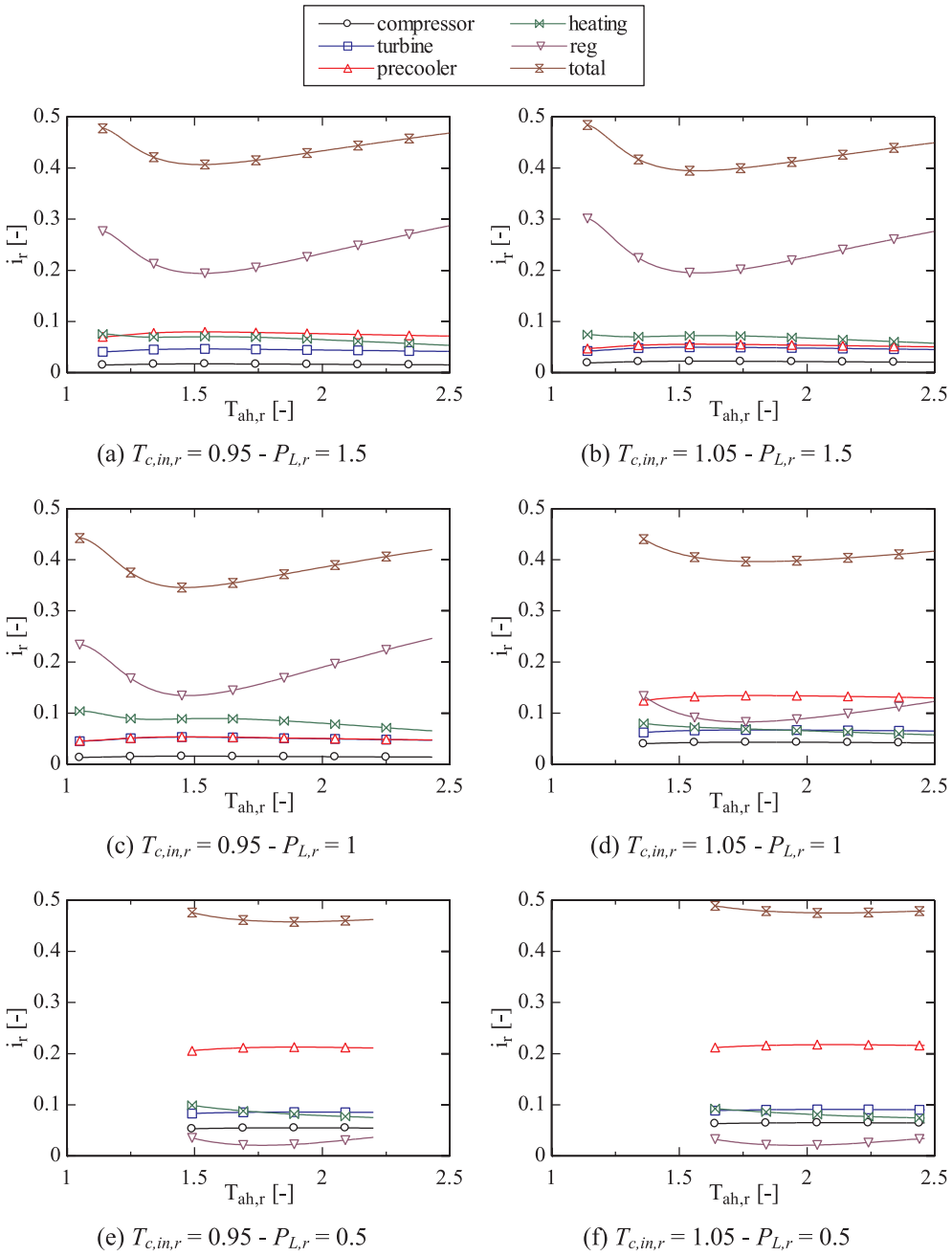

Fig. 13. Irreversibilities, *i*, as a function of additional-heat temperature, T_{ah}, in multi-heating pericritical cycles with different compressor inlet temperatures and low-side pressures.

an increase in regenerator irreversibility that lowers the exergy efficiency. However, if an additional heat is supplied (multi-heating cycle), the regenerator irreversibility may be reduced together with the precooler irreversibility. The result is that the optimum low-side pressure for the multi-heating cycle is greater than the optimum low-side pressure for the simple cycle. This pressure is close to the discontinuity line.

The greatest benefit of multi-heating is obtained in cycles with compressor inlet pressure above the discontinuity line due to the greater regeneration irreversibility. Fig. 15 shows the relative increment in exergy efficiency of multi-heating cycle with respect to simple cycle. The results are represented as a function of low-side pressure for the compressor inlet temperatures $T_{c,in,r}$ = 0.95 and $T_{c,in,r}$ = 1.05. The maximum relative increment is found at low-side pressures just above the corresponding discontinuity line (which depends on the compressor inlet temperature).

The relative increment of a multi-heating cycle with compressor inlet temperature $T_{c,in,r}$ = 1.05 and low-side pressure $P_{L,r}$ = 1.45 is $\Delta\eta_{ex}$ = 0.17. However, the relative increment between the maximum efficiency of multi-heating cycle and the maximum efficiency of simple cycle at this temperature is $\Delta\eta_{ex}$ = 0.1, since the optimum low-side pressures of these cycles are different (see Fig. 14). In the case of compressor inlet temperature $T_{c,in,r}$ = 0.95, the relative increment between the maximum efficiency of multi-heating cycle and simple cycle is $\Delta\eta_{ex}$ = 0.19.

Previous calculations have analysed the cycles with compressor inlet temperatures $T_{c,in,r}$ = 0.95 and $T_{c,in,r}$ = 1.05. Fig. 16 shows the influence of the compressor inlet temperature, $T_{c,in}$, in cycles with high-pressure side $P_{H,r}$ = 3. The low-side pressure is optimized in each case to maximize the exergy efficiency. Exergy efficiency and optimum low-side pressure side are represented.

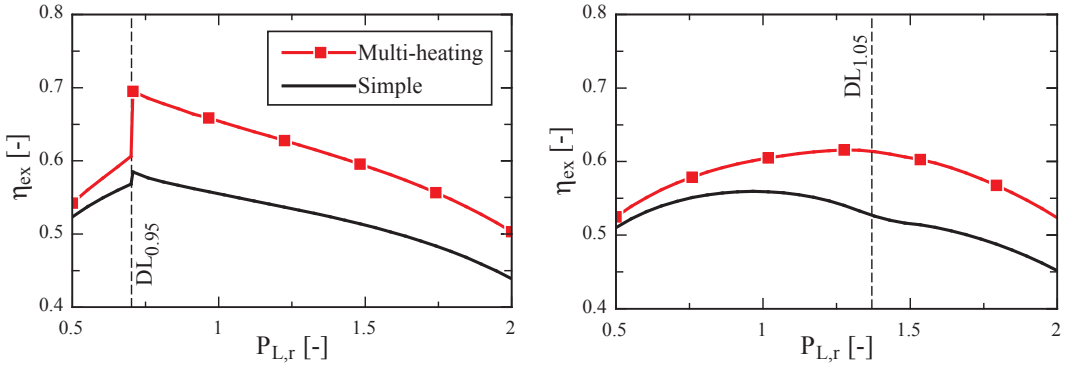

Fig. 14. Exergy efficiency, η_{ex}, of simple and multi-heating cycles as a function of low-pressure side, $P_{L,r}$. The compressor inlet temperatures are (a) $T_{c,in,r} = 0.95$ and (b) $T_{c,in,r} = 1.05$.

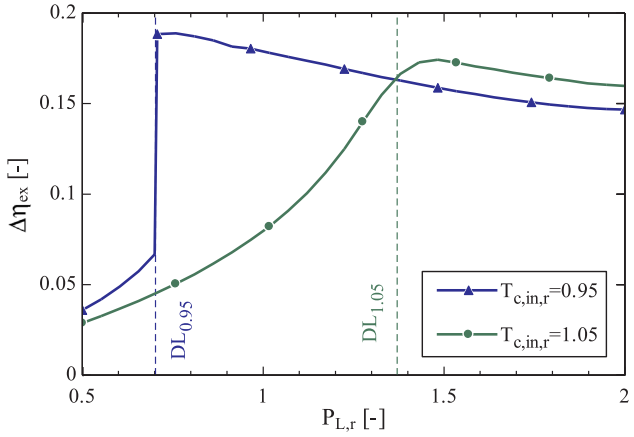

Fig. 15. Relative increment of exergetic efficiency, $\Delta\eta_{ex}$, of multi-heating cycles as a function of low-pressure side, $P_{L,r}$.

The lower the compressor inlet temperature, the higher the exergy efficiency is. Note that the Carnot factor is the same in all cycles. Thus, the difference in efficiency is due to the distribution of irreversibilities.

For low compressor inlet temperatures ($T_{c,in,r} < 0.98$), the optimum low-side pressure is just above the discontinuity line. This means low precooler irreversibility but high regenerator irreversibility. In simple cycles, the low precooler irreversibility outweighs the high regenerator irreversibility. In multi-heating cycles, the regeneration irreversibility is reduced, which results in a cycle with low precooler irreversibility and low regenerator irreversibility. When the compressor inlet temperature is $T_{c,in,r} < 0.98$, the exergy efficiency of multi-heating cycles is 18% greater than the efficiency of simple cycles.

For simple cycles with compressor inlet temperatures between $T_{c,in,r} = 0.98$ and $T_{c,in,r} = 1.1$, the low-side pressure is below the discontinuity line. The precooler irreversibility below the discontinuity line is greater than above it, but the regeneration irreversibility is low. In multi-heating cycles, the regeneration irreversibility may be reduced, allowing higher low-side pressures closer to the discontinuity line to increase the exergy efficiency.

The optimum low-side pressure and the exergy efficiency are ruled by the discontinuity line. The difference in efficiency between multi-heating and simple cycles is greater when the low-side pressure is above the discontinuity line, i.e., at temperatures below $T_{c,in,r} = 0.98$. In these cases, the exergy efficiency of multi-heating cycles is 18% greater than the efficiency of simple cycles. The efficiency gain of multi-heating decreases at higher temperatures. The lowest relative increase is 7%, which occurs at $T_{c,in,r} = 1.1$.

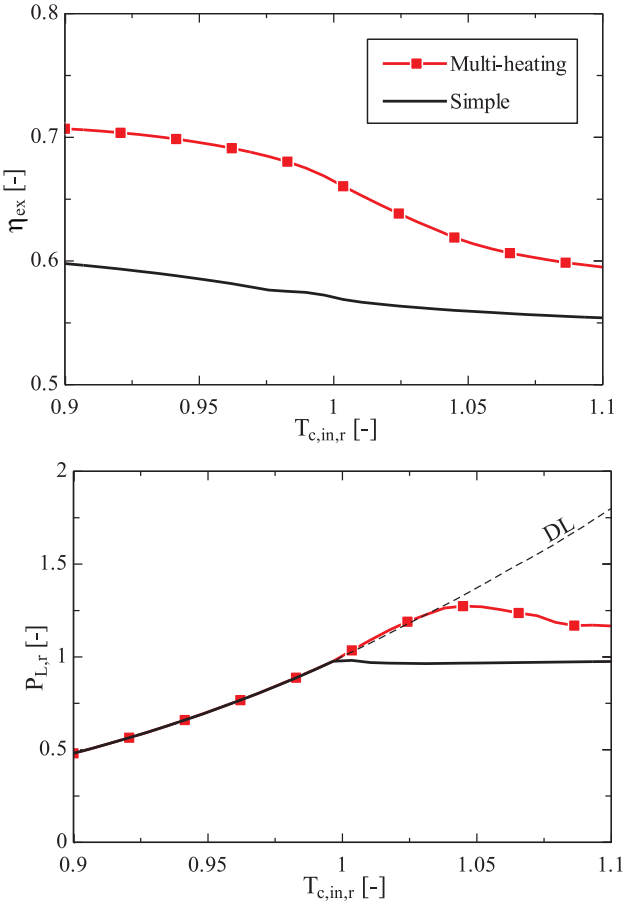

Fig. 16. Exergy efficiency, η_{ex}, and low-side pressure, $P_{L,r}$, of simple and multi-heating cycle as a function of the compressor inlet temperature, $T_{c,in,r}$.

4.2. High-side pressure

Previous calculations have set the high-side pressure to $P_{H,r} = 3$. This section analyses the influence of the high-side pressure in the exergy efficiency of multi-heating cycles. Fig. 17 shows precooler, regenerator and total irreversibilities of simple and multi-heating cycles for three different high-side pressures: $P_{H,r} = 5$, $P_{H,r} = 3$ and $P_{H,r} = 1$. Only precooler and regenerator irreversibilities are represented since they have shown to be the most relevant ones in the analysis of previous section. The compressor inlet temperature is $T_{c,in,r} = 0.95$. Note that the behavior would be similar with $T_{c,in,r} = 1.05$, except that with softer

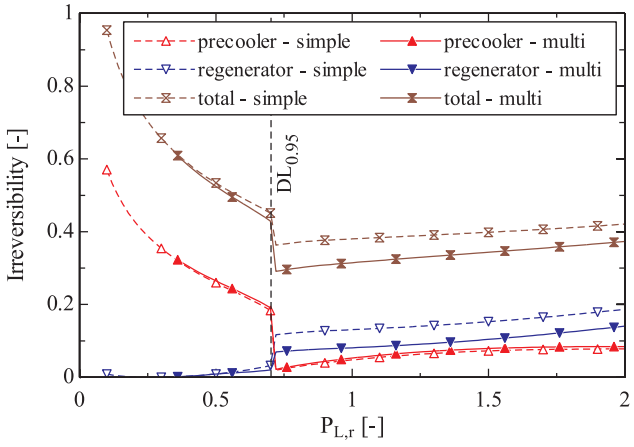

(a) $P_{H,r} = 5$

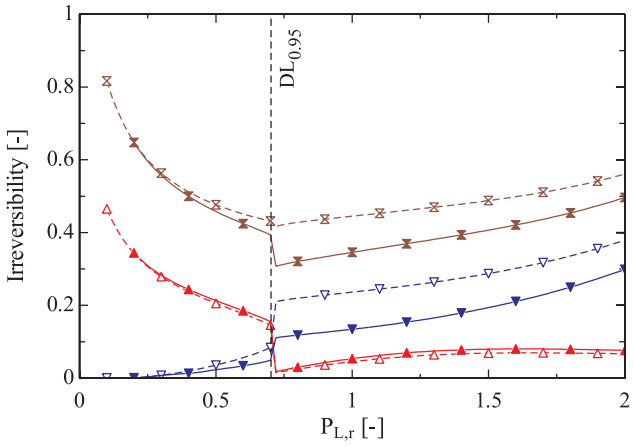

(b) $P_{H,r} = 3$

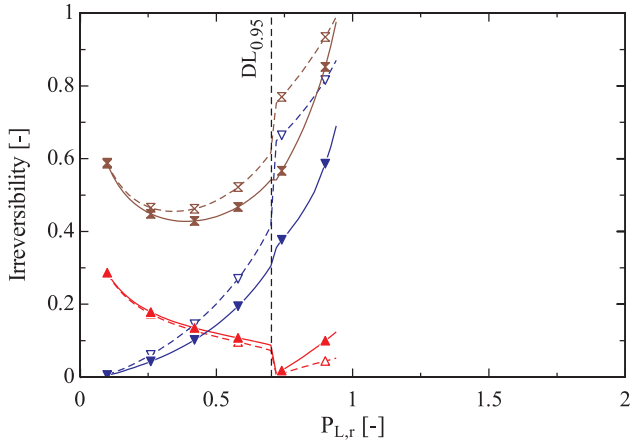

(c) $P_{H,r} = 1$

Fig. 17. Irreversibilities of simple (dashed lines) and multi-heating (continuous lines) cycle as a function of low-side pressure, $P_{L,r}$, for high-side pressures (a) $P_{H,r} = 5$, (b) $P_{H,r} = 3$ and (c) $P_{H,r} = 1$.

variations around the discontinuity line.

The regenerator irreversibility of simple cycles tends to one when the low-side pressure is very close to the high-side pressure. This can be appreciated in Fig. 17c when $P_{L,r} \approx P_{H,r} = 1$. Lowering the low-side pressure involves a reduction of regenerator irreversibility. This irreversibility decreases uniformly till the discontinuity line. At low-side pressure just above the discontinuity line, the greater the distance between high-side pressure and discontinuity line the smaller the regenerator irreversibility is. For example, the regenerator irreversibility is $i_r = 0.12$ when $P_{H,r} = 5$ ($P_H/P_{DL} = 7.1$) and $i_r = 0.65$ when $P_{H,r} = 1$ ($P_H/P_{DL} = 1.4$).

The greater the regenerator irreversibility in simple cycles, the greater the decrease of this irreversibility is by means of multi-heating. In this way, the regenerator irreversibility in Fig. 17c is reduced from 0.65 to 0.35 and in Fig. 17a from 0.12 to 0.07. In spite of the big reduction in Fig. 17c, the regenerator irreversibility of the simple cycle is that high that it is still high in the multi-heating cycle.

The precooler irreversibility is almost null at low-side pressures just above the discontinuity line. Therefore, cycles with low regenerator irreversibility at these pressures present the lowest total irreversibilities. This is the case of cycles in Fig. 17a and b, in which multi-heating reduces even more the total irreversibility.

When the low-side pressure is lowered below the discontinuity line, precooler irreversibility increases and regenerator irreversibility decreases even more. The benefit of multi-heating is almost null in these cases. In Fig. 17a and b, the increase of precooler irreversibility makes grow the total irreversibility, making it higher than the total irreversibility obtained above the discontinuity line. In Fig. 17c, the decrease of regenerator irreversibility outweighs the increase of precooler irreversibility when the low-side pressure is below and close to the discontinuity line. Thus, the minimum total irreversibility is found at low-side pressures below the discontinuity line.

The optimum low-side pressure to minimize the total irreversibility depends on the high-side pressure and the compressor inlet temperature. Fig. 18 shows exergy efficiency, η_{ex}, and optimum low-side pressure, $P_{L,r}$, of simple and multi-heating cycle as a function of high-side pressure for compressor inlet temperatures $T_{c,in,r.} = 0.95$ and $T_{c,in,r} = 1.05$. Fig. 18a and b present a similar behavior ruled by the discontinuity line. The main difference is that variations are more abrupt in Fig. 18a.

Low-side pressures below the discontinuity line belong to cycles with high-side pressures close to the discontinuity line. The small range of pressures between high-side pressure and discontinuity line implies that the regeneration irreversibility is too high just above the discontinuity line. Thus, the optimum low-side pressures are below the discontinuity line where the regeneration irreversibility is lower. This is the case of simple cycles with high-side pressure $P_{H,r} < 2.3$ ($P_H/P_{DL,0.95} < 3.2$) in Fig. 18a and $P_{H,r} < 4.2$ ($P_H/P_{DL,1.05} < 3.1$) in Fig. 18b.

Supplying additional heats reduce the regenerator irreversibility. Thus, multi-heating increases the optimum low-side pressure of some of the simple cycles from below the discontinuity line to just above it. For example, when the high-side pressure is $P_{H,r} = 1.4$ in Fig. 18a, the optimum low-side pressure rises from $P_{L,r} = 0.47$ in the simple cycle to $P_{L,r} = P_{DL} = 0.7$ in the multi-heating cycle.

The difference in efficiency between multi-heating and simple cycles is small when the low-side pressure is below the discontinuity line in both cases. This occurs at low high-side pressures. The difference in efficiency grows when the optimum low-side pressure of multi-heating cycle approaches the discontinuity line or gets over it. In these cases, multi-heating reduces the regenerator irreversibility resulting in a lower total irreversibility. However, when the high-side pressure is too high, the regenerator irreversibility is already low in simple cycles, which means that the benefit of multi-heating is smaller. Therefore, there is a high-side pressure for which multi-heating cycles obtain the maximum benefit. The maximum relative increment of exergy efficiency is 20.8% at $P_{H,r} = 2.7$ in Fig. 18a and 12.1% at $P_{H,r} = 3.7$ in Fig. 18b.

The influence of the compressor inlet temperature and the high pressure has been studied separately to understand its behaviour. However, the exergy efficiency depends on both temperature and pressure at the same time. Fig. 19 shows the exergy efficiency of simple cycles (top) and multi-heating cycles (bottom) as a function of high-

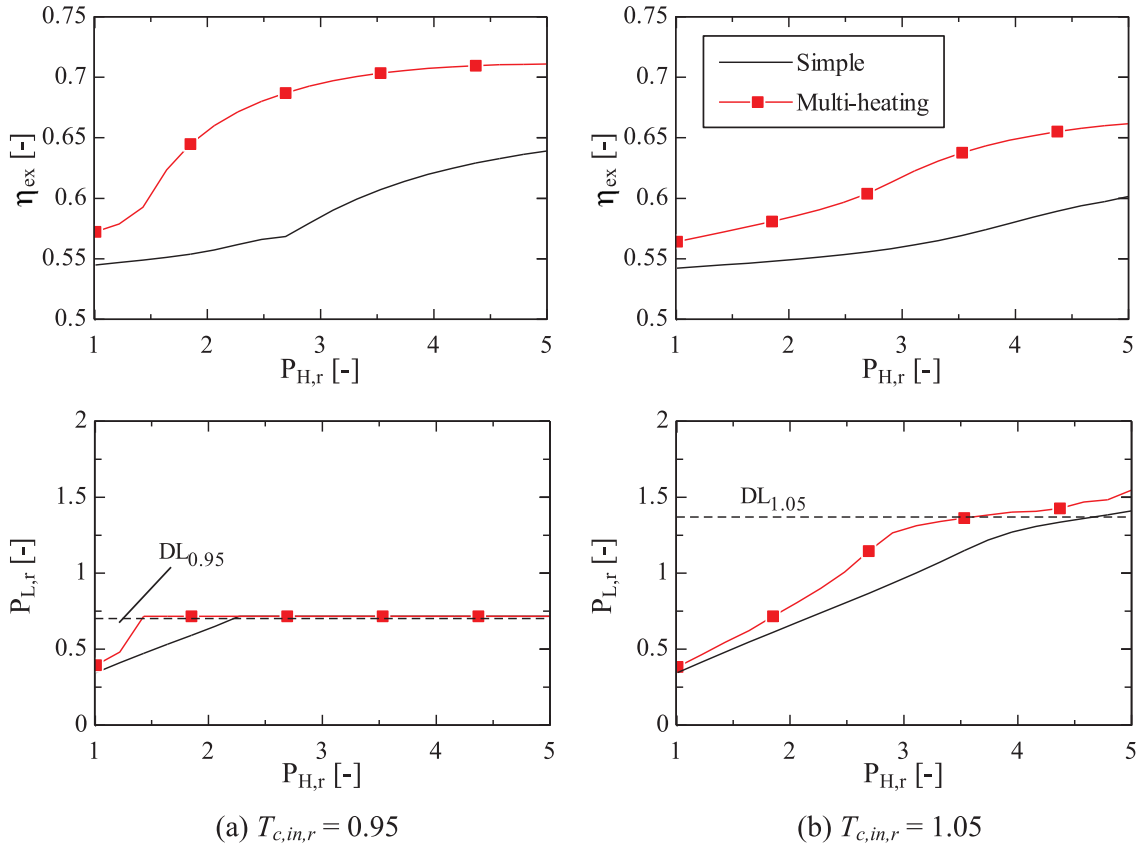

Fig. 18. Exergy efficiency, η_{ex}, and low-side pressure, $P_{L,r}$, of simple and multi-heating cycle as a function of high-side pressure, $P_{H,r}$, for compressor inlet temperatures (a) $T_{c,in,r}$. = 0.95 and (b) $T_{c,in,r}$ = 1.05.

pressure side, $P_{H,r}$, and compressor inlet temperature, $T_{c,in,r}$. The efficiency increases by raising the high-side pressure and lowering the compressor inlet temperature in both cases.

The efficiencies of multi-heating cycles are greater than the efficiencies of simple cycles. The potential of multi-heating cycles can be analysed by calculating the relative increase of exergy efficiency with respect to simple cycles. Fig. 20 shows this relative increase, $\Delta\eta_{ex}$, as a function of high-pressure side, $P_{H,r}$, and compressor inlet temperature, $T_{c,in,r}$.

The lowest relative increase is obtained around the critical point ($T_{c,in,r}$ = 1 and $P_{H,r}$ = 1). These cycles work below the discontinuity line, which means that the advantages of multi-heating can barely be used. Increasing the compressor inlet temperature without raising the high-side pressure ($T_{c,in,r}$ > 1 and $P_{H,r}$ = 1) hardly affects the relative increase because the cycle is still working far below the discontinuity line. The solution to take advantage of multi-heating is either by raising the high pressure ($T_{c,in,r}$ = 1 and $P_{H,r}$ > 1) or by decreasing the compressor inlet temperature ($T_{c,in,r}$ < 1 and $P_{H,r}$ = 1). In both cases, the purpose is to achieve that the compressor works above the discontinuity line or close to it.

The cycle needs a minimum range of pressures between the high-side pressure and the discontinuity line to take full advantage of multi-heating. This minimum range of pressures corresponds approximately to a P_H/P_{DL} = 2. The isoexergetic line $\Delta\eta_{ex}$ = 10% has approximately this pressure ratio. The relative increase of efficiency grows up to a maximum by raising the high-side pressure above this isoexergetic line. The value of this maximum and its high-side pressure depend on the compressor inlet temperature. The higher the compressor inlet temperature the lower the value of the maximum increment $\Delta\eta_{ex}$ and the higher the high-side pressure. The maximum efficiency increment in Fig. 20 is $\Delta\eta_{ex}$ = 24%, obtained at high-side pressure $P_{H,r}$ = 2.7 and compressor inlet temperature $T_{c,in,r}$ = 0.9.

4.3. Fluid

Previous results have been obtained with the thermodynamic properties of CO_2. Other fluids with similar thermodynamic properties although with different critical pressure and critical temperature will show similar results. Moreover, the main tendencies marked by the discontinuity line are expected to be similar even with different thermodynamic properties.

R125 is a fluid with thermodynamic properties very different from those of CO_2 [32]. The thermodynamic properties of R125 are used to calculate the relative increase in exergy efficiency of multi-heating cycles with respect to simple cycles. Fig. 21 shows the results as a function of high-pressure side and compressor inlet temperature in the same way than in Fig. 20. Although the values obtained with the thermodynamic properties of CO_2 in Fig. 20 are different, the same main tendencies can be observed in Fig. 21, in spite of using different thermodynamic properties.

This paper focuses on the analysis of multi-heating cycles from a thermodynamic point of view. The purpose is to abstract the analysis from the fluid as much as possible. The results show the behavior of fluids with specific thermodynamic properties, but with undetermined critical temperature and critical pressure. In this way, a fluid with low critical pressure can more easily reach high reduced high-side pressures and, therefore, increase the cycle efficiency. And a fluid with high critical temperature can more easily reach lower reduced compressor inlet temperatures and, therefore, obtain greater efficiency increments from multi-heating.

For example, consider critical pressure and critical temperature from CO_2 and R125 (see Table 4.1). A compressor inlet temperature $T_{c,in}$ = 50 °C corresponds to $T_{c,in,r}$ = 1.06 for CO_2 and $T_{c,in,r}$ = 0.95 for R125. Multi-heating cycles with both fluids have great benefits at high-side pressure $P_{H,r}$ = 3. The relative increase in exergy efficiency is

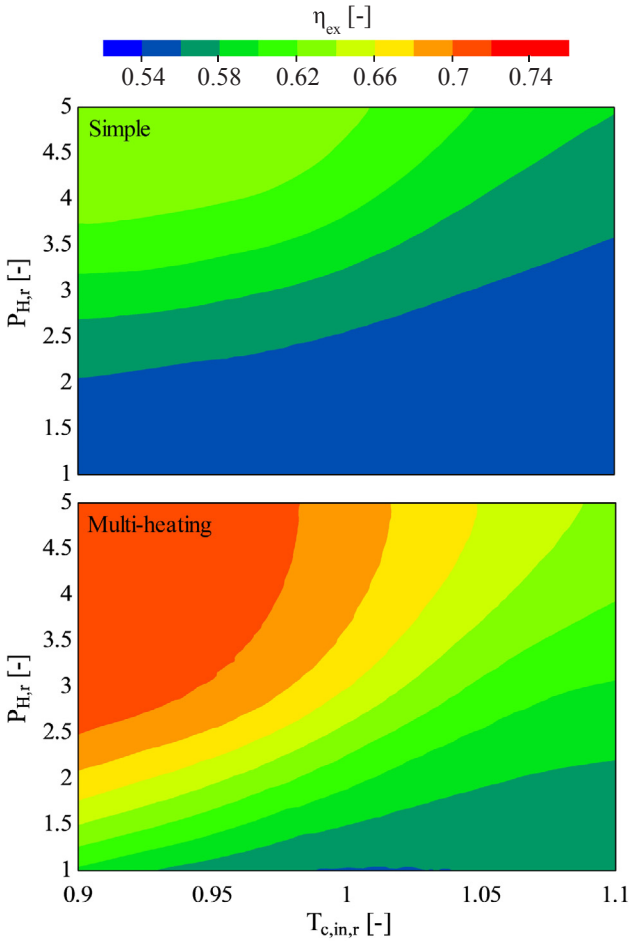

Fig. 19. Exergy efficiency, η_{ex}, as a function of the high-pressure side, $P_{H,r}$, and compressor inlet temperature, $T_{c,in,r}$, in simple cycle (top) and multi-heating cycle (bottom).

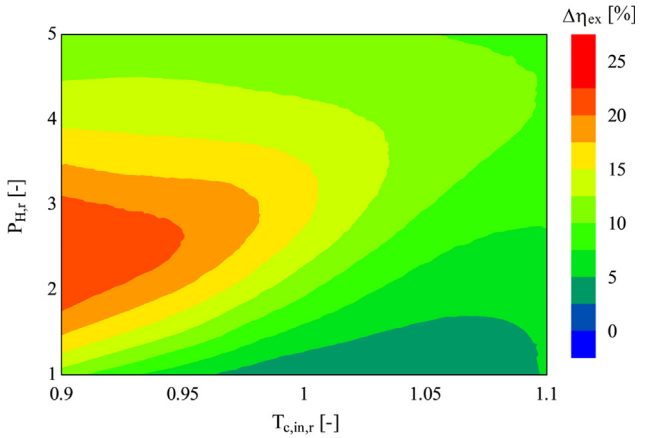

Fig. 20. Relative increase in exergy efficiency, $\Delta\eta_{ex}$, of multi-heating cycles as a function of the high-pressure side, $P_{H,r}$, and compressor inlet temperature, $T_{c,in,r}$.

$\Delta\eta_{ex}$ = 9% for the cycle with CO_2 and $\Delta\eta_{ex}$ = 15% for the cycle with R125. The relative increase is greater with R125 due to the lower reduced compressor inlet temperature in the cycle. Moreover, the lower critical pressure of R125 involves that the high-side pressure of the cycle with this fluid is lower. In the case of the cycle with R125 this pressure would be P_H = 10.8 MPa and in the case of the cycle with CO_2 P_H = 22.2 MPa.

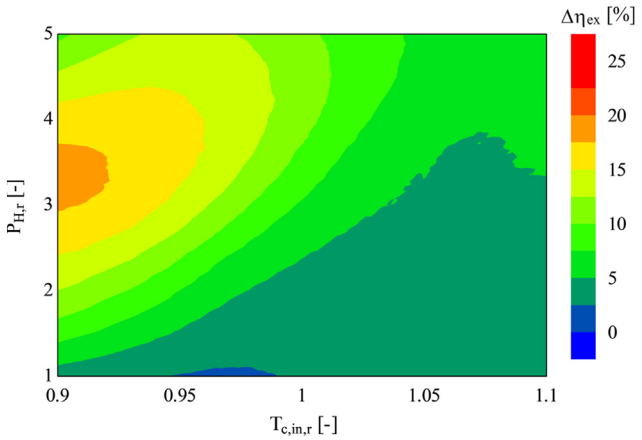

Fig. 21. Relative increase in exergy efficiency, $\Delta\eta_{ex}$, of multi-heating with thermodynamic properties of R125 as a function of high-pressure side, $P_{H,r}$, and compressor inlet temperature, $T_{c,in,r}$.

Table 4.1
Critical temperature and pressure of fluids CO_2 and R125.

Parameter	CO_2	R125
Critical temperature, T_{cr}	31 °C	66 °C
Critical pressure, P_{cr}	7.4 MPa	3.6 MPa

Of course, the working fluid in a pericritical cycle will not be selected based uniquely on the critical point. For example, CO_2 is commonly used in supercritical cycles due to, among other things, its stability and relative inertness at high temperatures [4], while R125 has the drawback of thermal decomposition at temperatures below 400–450 °C [33]. Anyway, the purpose of this paper is not to select the best fluid for pericritical cycles, but to help in the selection. The analysis of alternative fluids for pericritical cycles is a current topic in research [34]. Some researchers [35] look for mixtures with CO_2 with the purpose of varying the critical point. The results of this paper may help in the selection of the pursue optimum fluid from a thermodynamic point of view.

4.4. Application

Although the purpose of this work is to abstract the analysis from the fluid, it is worth to analyse a practical example with CO_2, since it is the most popular fluid for supercritical conditions. The parameters used to define the CO_2 cycle are shown in Table 4.2. These parameters have been previously used by Kim et al. [6] to compare the exergy efficiency of simple and multi-heating CO_2 cycles. The reduced values of these parameters are very similar to the ones used in the rest of the paper. Thus, the results shown in this paper can be used as a guidance in the optimization of this cycle. For example, we can appreciate from Fig. 20 that these cycle conditions have a great potential to take advantage of multi-heating.

Table 4.2
Parameters to analyze pericritical CO_2 cycles [6].

Parameter	Value	Reduced value
High-side pressure, P_H	20 MPa	2.71
Low-side pressure, P_L	5.73 MPa	0.78
Compressor inlet temperature, $T_{c,in}$	20 °C	0.96
Turbine inlet temperature, $T_{t,in}$	600 °C	2.88
Additional-heat temperature, T_{ah}	112 °C	1.27
Compressor efficiency, η_c	0.9	–
Turbine efficiency, η_t	0.9	–
IHX effectiveness, ε	0.95	–

The low-side pressure from Table 4.2 is the optimum value to maximize the exergy efficiency. However, the additional-heat temperature is not. The additional-heat temperature analysed by Kim et al. [6] is $T_{ah} = 112$ °C, while the optimum one is $T_{ah} = 156$ °C. In this way, the exergy efficiency obtained with the former temperature is $\eta_{ex} = 0.71$ and the exergy efficiency obtained with the latter temperature $\eta_{ex} = 0.73$. Anyway, both are greater than the efficiency of the simple cycle $\eta_{ex} = 0.63$.

The compressor inlet temperature will determine the benefit of multi-heating, and sometimes the compressor inlet temperature from Table 4.2 may not be achieved. Thus, other studies analyse power cycles at higher compressor inlet temperatures [36]. For example, a common value for this temperature in Concentrating Solar Power plants is $T_{c,in} = 50$ °C since the CO_2 is cooled by air at temperatures between 30 °C and 40 °C. If the conditions from Table 4.2 are used with compressor inlet temperature $T_{c,in} = 50$ °C, the maximum exergy efficiency in simple and multi-heating cycles would be $\eta_{ex} = 0.61$ and $\eta_{ex} = 0.66$, respectively. The benefit of multi-heating in this case is reduced to the half, and the extra complexity of the multi-heating cycle may not compensate the increase in efficiency.

The use of multi-heating cycles at high compressor inlet temperatures will require the use of other fluids with higher critical temperature. R125 was an example of fluid with these characteristics, but the maximum temperature in the cycle would be limited to temperatures below 400–450 °C. Other fluids mixtures with CO_2 with higher critical point could be an option.

5. Conclusions

While a single heat source supplies the thermal power in simple regenerative cycles, additional heat sources at lower temperatures supply part of this power in multi-heating cycles. Supplying heat at lower temperature during the regeneration reduces the regenerator irreversibility. Multi-heating cycles achieve exergy efficiencies up to 24% greater than in simple cycles by reducing these irreversibilities.

This paper compares multi-heating cycles and simple cycles with the compressor working in the pericritical region. The analysis focuses on multi-heating cycles with one additional heat (i.e. two heats in total: primary and additional heat) since the results show that the greater exergy efficiency resulting from increasing the number of additional heats does not seem to compensate the greater complexity.

The benefit of multi-heating cycles is analyzed for cycles with the same Carnot efficiency and different compressor positions in the thermodynamic diagram. The discontinuity line (set of the coexistence line and the Widom line) guides the cycle characterization. Simple cycles with the compressor at pressures above this line have small precooler irreversibilities and big regenerator irreversibilities. Multi-heating cycles in the same conditions reduce regenerator irreversibilities and keep precooler irreversibilities low, resulting in higher exergy efficiencies than in simple cycles.

The conditions for the compressor to work above the discontinuity line depend on cycle limiting pressures and compressor inlet temperature. The greatest benefit of multi-heating cycles is found when the pressure ratio between the high-side pressure and the discontinuity line is above two. The lower the compressor inlet temperature, the lower the high-side pressure has to be to fulfill this requirement. The optimum reduced high-side pressures are found to vary between 2.7 and 4.3 in the range of reduced compressor inlet temperatures 0.9 to 1.1. Raising the high-side pressure above these values involves an increase of exergy efficiency in simple and multi-heating cycles, but the benefit of multi-heating decreases since the regenerator irreversibility is already small in simple cycles and, therefore, multi-heating cycles can hardly reduce it.

The results of this paper are shown as a function of reduced temperature and reduced pressure. The purpose is to extrapolate the tendencies obtained with the thermodynamic properties of CO_2 to other fluids. The calculations done with R125 show that the main tendencies are similar. These tendencies can help to estimate as a first approximation the advantages of multi-heating cycles depending on the critical pressure and the critical temperature, and so help in the search of optimum working fluids. For example, while multi-heating highly increases the exergy efficiency of cycles with CO_2 at low compressor inlet temperatures, it hardly does it when the cooling cannot achieve these low temperatures. Thus, other fluids with higher critical temperature must be used in these cases. Future work will focus on the analysis of the main characteristics that a fluid should have in order to achieve high efficiencies in multi-heating pericritical cycles. Moreover, different fluids (including mixtures) able to work in pericritical cycles will be analysed.

Declaration of Competing Interest

The authors declare that they have no known competing financial interests or personal relationships that could have appeared to influence the work reported in this paper.

Acknowledgments

Technical discussions with other members of the research group “Grupo de Investigaciones Termoenergéticas” from the Universidad Politécnica de Madrid were essential for this work. The authors wish to thank to “Comunidad de Madrid” and European Structural Funds for their financial support to ACES2030-CMproject(S2018/EMT-4319).

References

[1] Y. Ahn, S.J. Bae, M. Kim, S.K. Cho, S. Baik, J.I. Lee, J.E. Cha, Review of supercritical CO2 power cycle technology and current status of research and development, Nucl. Eng. Technol. 47 (2015) 647–661, https://doi.org/10.1016/j.net.2015.06.009.
[2] A. Bejan, Advanced Engineering Thermodynamics, third ed., John Wiley & Sons, Danvers, USA, 2006.
[3] E.G. Feher, The supercritical thermodynamic power cycle, Energy Convers. 8 (1968) 85–90, https://doi.org/10.1016/0013-7480(68)90105-8.
[4] V. Dostal, A Supercritical Carbon Dioxide Cycle for Next Generation Nuclear Reactors, PhD Thesis Massachusetts Institute of Technology, 2004.
[5] M.-J. Li, H.-H. Zhu, J.-Q. Guo, K. Wang, W.-Q. Tao, The development technology and applications of supercritical CO2 power cycle in nuclear energy, solar energy and other energy industries, Appl. Therm. Eng. 126 (2017) 255–275, https://doi.org/10.1016/J.APPLTHERMALENG.2017.07.173.
[6] Y.M. Kim, C.G. Kim, D. Favrat, Transcritical or supercritical CO2 cycles using both low- and high-temperature heat sources, Energy 43 (2012) 402–415, https://doi.org/10.1016/j.energy.2012.03.076.
[7] G. Angelino, Carbon dioxide condensation cycles for power production, J. Eng. Gas Turbines Power. 90 (1968) 287–295, https://doi.org/10.1115/1.3609190.
[8] A.A. AlZahrani, I. Dincer, Thermodynamic analysis of an integrated transcritical carbon dioxide power cycle for concentrated solar power systems, Sol. Energy 170 (2018) 557–567, https://doi.org/10.1016/J.SOLENER.2018.05.071.
[9] G. Shu, Z. Yu, H. Tian, P. Liu, Z. Xu, Potential of the transcritical Rankine cycle using CO2-based binary zeotropic mixtures for engine’s waste heat recovery, Energy Convers. Manag. 174 (2018) 668–685, https://doi.org/10.1016/J.ENCONMAN.2018.08.069.
[10] P. Morrone, A. Algieri, T. Castiglione, Hybridisation of biomass and concentrated solar power systems in transcritical organic Rankine cycles: a micro combined heat and power application, Energy Convers. Manag. 180 (2019) 757–768, https://doi.org/10.1016/J.ENCONMAN.2018.11.029.
[11] G. Angelino, Real gas effects in carbon dioxide, ASME Publ., 1969, pp. 1–12.
[12] Y. Ma, Z. Liu, H. Tian, A review of transcritical carbon dioxide heat pump and refrigeration cycles, Energy 55 (2013) 156–172, https://doi.org/10.1016/J.ENERGY.2013.03.030.
[13] J.H. Song, H.Y. Kim, H. Kim, Y.Y. Bae, Heat transfer characteristics of a supercritical fluid flow in a vertical pipe, J. Supercrit. Fluids 44 (2008) 164–171, https://doi.org/10.1016/J.SUPFLU.2007.11.013.
[14] J. Sarkar, Review and future trends of supercritical CO2 Rankine cycle for low-grade heat conversion, Renew. Sustain. Energy Rev. 48 (2015) 434–451, https://doi.org/10.1016/J.RSER.2015.04.039.
[15] F. Crespi, G. Gavagnin, D. Sánchez, G.S. Martínez, Supercritical carbon dioxide cycles for power generation: a review, Appl. Energy 195 (2017) 152–183, https://doi.org/10.1016/J.APENERGY.2017.02.048.
[16] L.F. González-Portillo, J. Muñoz-Antón, J.M. Martínez-Val, Thermodynamic mapping of power cycles working around the critical point, Energy Convers. Manag. 192 (2019) 359–373, https://doi.org/10.1016/j.enconman.2019.04.022.
[17] C. Coquelet, D. Ramjugernath, Phase Diagrams in Chemical Engineering:

Application to Distillation and Solvent Extraction, in: Adv. Chem. Eng., 2012. https://doi.org/10.5772/33632.
[18] F. Sciortino, P. Poole, U. Essmann, H. Stanley, Line of compressibility maxima in the phase diagram of supercooled water, Phys. Rev. E 55 (1997), https://doi.org/10.1103/PhysRevE.55.727.
[19] D. Banuti, M. Raju, P.C. Ma, M. Ihme, J.-P. Hickey, Seven questions about supercritical fluids - towards a new fluid state diagram, in: 55th AIAA Aerosp. Sci. Meet., 2017. https://doi.org/10.2514/6.2017-1106.
[20] I.L. Pioro, C.O. Zvorykin, Thermophysical properties of fluids at subcritical and critical/supercritical conditions, in: Handb. Gener. IV Nucl. React., Elsevier, 2016, pp. 771–794. https://doi.org/10.1016/B978-0-08-100149-3.15003-7.
[21] G.D. Pérez-Pichel, J.I. Linares, L.E. Herranz, B.Y. Moratilla, Thermal analysis of supercritical CO2 power cycles: assessment of their suitability to the forthcoming sodium fast reactors, Nucl. Eng. Des. 250 (2012) 23–34, https://doi.org/10.1016/J.NUCENGDES.2012.05.011.
[22] J. Sarkar, Second law analysis of supercritical CO2 recompression Brayton cycle, Energy 34 (2009) 1172–1178, https://doi.org/10.1016/j.energy.2009.04.030.
[23] M.T. Dunham, B.D. Iverson, High-efficiency thermodynamic power cycles for concentrated solar power systems, Renew. Sustain. Energy Rev. 30 (2014) 758–770, https://doi.org/10.1016/j.rser.2013.11.010.
[24] J. Syblik, L. Vesely, S. Entler, J. Stepanek, V. Dostal, Analysis of supercritical CO2 Brayton power cycles in nuclear and fusion energy, Fusion Eng. Des. In Press (2019), https://doi.org/10.1016/J.FUSENGDES.2019.02.119.
[25] J. Dyreby, Modeling the Supercritical Carbon Dioxide Brayton Cycle with Recompression, PhD Thesis The University of Wisconsin, Madison, 2014.
[26] J. Muñoz, J.M. Martinez-Val, A. Ramos, Thermal regimes in solar-thermal linear collectors, Sol. Energy 85 (2011) 857–870, https://doi.org/10.1016/j.solener.2011.02.004.
[27] R.V. Padilla, Y.C. Soo Too, R. Benito, W. Stein, Exergetic analysis of supercritical CO2 Brayton cycles integrated with solar central receivers, Appl. Energy 148 (2015) 348–365, https://doi.org/10.1016/j.apenergy.2015.03.090.
[28] A. Müller, L. Kranzl, P. Tuominen, E. Boelman, M. Molinari, A.G. Entrop, Estimating exergy prices for energy carriers in heating systems: country analyses of exergy substitution with capital expenditures, Energy Build. 43 (2011) 3609–3617, https://doi.org/10.1016/J.ENBUILD.2011.09.034.
[29] S. Klein, Engineering Equation Solver (EES), 1992.
[30] E.D. Sánchez Villafana, J.P. Vargas Machuca Bueno, Thermoeconomic and environmental analysis and optimization of the supercritical CO2 cycle integration in a simple cycle power plant, Appl. Therm. Eng. 152 (2019) 1–12. https://doi.org/10.1016/J.APPLTHERMALENG.2019.02.052.
[31] L.F. González Portillo, A New Concept in Thermal Engineering Optimization: the Pericritical Cycle with Multi-Heating and its Application to Concentrating Solar Power, PhD Thesis, Universidad Politécnica de Madrid, 2019. https://doi.org/10.20868/UPM.thesis.56492.
[32] A. Rovira, J. Muñoz-Antón, M.J. Montes, J.M. Martínez-Val, Optimization of Brayton cycles for low-to-moderate grade thermal energy sources, Energy 55 (2013) 403–416, https://doi.org/10.1016/j.energy.2013.03.094.
[33] C.M. Invernizzi, Prospects of mixtures as working fluids in real-gas Brayton cycles, Energies 10 (2017) 1–15, https://doi.org/10.3390/en10101649.
[34] L. Hu, D. Chen, Y. Huang, L. Li, Y. Cao, D. Yuan, J. Wang, L. Pan, Investigation on the performance of the supercritical Brayton cycle with CO2-based binary mixture as working fl uid for an energy transportation system of a nuclear reactor, Energy 89 (2015) 874–886, https://doi.org/10.1016/j.energy.2015.06.029.
[35] J. Guo, M. Li, J. Xu, J. Yan, K. Wang, Thermodynamic performance analysis of different supercritical Brayton cycles using CO2-based binary mixtures in the molten salt solar power tower systems, Energy 173 (2019) 785–798, https://doi.org/10.1016/j.energy.2019.02.008.
[36] M. Monjurul Ehsan, S. Duniam, J. Li, Z. Guan, H. Gurgenci, A. Klimenko, A comprehensive thermal assessment of dry cooled supercritical CO2 power cycles, Appl. Therm. Eng. 114645 (2019), https://doi.org/10.1016/J.APPLTHERMALENG.2019.114645.